International Journal of Engineering & Technology, 7 (4.36) (2018) 1428-1434

International Journal of Engineering & Technology

Website: www.sciencepubco.com/index.php/IJET

Research paper

State-feedback control with a full-state estimator for a cart-inverted pendulum system

Indrazno Siradjuddin[1], Zakiyah Amalia[1*], Erfan Rohadi[2], Budhy Setiawan[1], Awan Setiawan[1], Ratna Ika Putri[1], and Erni Yudaningtyas[3]

[1]State Polytechnic of Malang, Electrical Engineering Department, Malang, Indonesia
[2]State Polytechnic of Malang, Information Technology Department, Malang, Indonesia
[3]Brawijaya University, Electrical Engineering Department, Malang, Indonesia
**Corresponding author E-mail: zakiyah amalia@polinema.ac.id*

Abstract

A Cart Inverted Pendulum System is an unstable, nonlinear and underactuated system. This makes a cart inverted pendulum system used as a benchmark for testing many control method. A cart must occupy the desired position and the angle of the pendulum must be in an equilibrium point. System modeling of a cart inverted pendulum is important for controlling this system, but modeling using assumptions from state-feedback control is not completely valid. To minimize unmeasured state variables, state estimators need to be designed. In this paper, the state estimator is designed to complete the state-feedback control to control the cart inverted pendulum system. The mathematical model of the cart inverted pendulum system is obtained by using the Lagrange equation which is then changed in the state space form. Mathematical models of motors and mechanical transmissions are also included in the cart inverted pendulum system modeling so that it can reduce errors in a real-time application. The state gain control parameter is obtained by selecting the weighting matrix in the Linear Quadratic Regulator (LQR) method, then added with the Leuenberger observer gain that obtained by the pole placement method on the state estimator. Simulation is done to determine the system performance. The simulation results show that the proposed method can stabilize the cart inverted pendulum system on the cart position and the desired pendulum angle.

Keywords: *Cart Inverted Pendulum; Lagrange Equation; LQR; State Estimator; State-Feedback Control*

1. Introduction

The cart inverted pendulum system is a very common system for testing many control methods such as PID[1], LQR[2], pole placement[3], fuzzy logic[4], genetic algorithms[5], LQG[6], etc. A normal pendulum that is a pendulum facing downward is a stable system because there is a gravitational force that will force the normal pendulum back to its starting position. Otherwise, the inverted pendulum or pendulum facing upwards is an unstable system. This system also has many problems such as nonlinear, underactuated, and complex systems. Controlling the inverted pendulum system is about the position and balance point of the pendulum[7], such as on two-wheeled self-balancing scooters, single-wheeled electric unicycles, humanoid robots[8], etc. This makes the researchers interested in developing this system to get better system performance. One of the control methods that commonly used to control this cart inverted pendulum system is the state feedback controller[9]. However, the use of the state feedback controller is not enough to represent all the states in the cart inverted pendulum system. A state observer[10] needs to be added to find out all the states in this system. This paper discusses the control of the inverted pendulum system cart using state feedback control with a full-state estimator. The parameters of state feedback control are obtained by the Linear Quadratic Regulator. The selection of the $\boldsymbol{Q}$ and R weighting matrix is done to get the best response. The addition of full-state estimator parameters with Leuenberger observer gain is done by the pole placement method with selecting the desired pole. The selection is done to get an optimal response with a minimum control signal. Mathematical models using mechanical transmission and dc motors are added to approach the real cart inverted pendulum system. The modeling of cart inverted pendulum system with the Lagrange equation and the state space representation of the inverted pendulum system cart are shown in chapter 2. The selection of state feedback parameters with Linear Quadratic Regulator and full-state observers with pole placement is shown in chapter 3. The simulation results are shown in chapter 4, and the last in chapter 5 there is a conclusion.

2. System Modeling

A cart inverted pendulum system is shown in Figure.1. The cart of cart inverted pendulum is moved along c-axis direction by DC motor. Belt and pulley are used in mechanical transmission to gain the torque of the actuator. The angular acceleration and the angular velocity of DC motor are controlled to get the acceleration and the velocity of the cart.

2.1. Lagranges Equation

In this cart inverted pendulum system, there is a force by DC motor that applied to the cart, f. This force affects the system output (x, θ). To control the system, Lagranges equation used to deriving a mathematical model of the cart inverted pendulum. The Lagranges Equation is the equation that combines the kinetic energy $\boldsymbol{K}$ and potential energy $\boldsymbol{P}$ of the system. Using the equalised coordinate $\boldsymbol{q} = \{q_1, \dots, q_i, \dots, q_n\}$ of the system, the mathematical

Copyright © 2018 Authors. This is an open access article distributed under the Creative Commons Attribution License, which permits unrestricted use, distribution, and reproduction in any medium, provided the original work is properly cited.

model of the system can be described. n is the total established equalised coordinate and q_i is an exempt degree of freedom from the system.

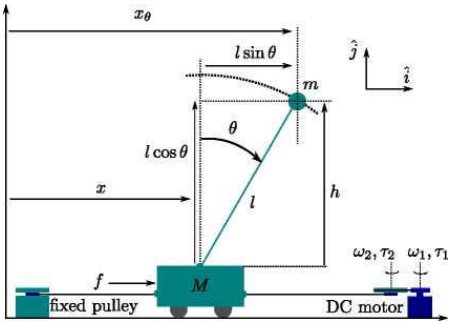


Fig. 1: System of a cart inverted pendulum

The Lagrangian equation $\boldsymbol{\mathcal{L}}$ can be described as

$$\boldsymbol{\mathcal{L}} = \boldsymbol{K}(\mathbf{q}, \dot{\mathbf{q}}) - \boldsymbol{P}(\mathbf{q}) \tag{1}$$

where the equalised coordinate $\mathbf{q}$ and the derivation of it $\dot{\mathbf{q}}$ are used in the function of kinematic energy. The equalised coordinate $\mathbf{q}$ used in the function of potential energy. The term of x and θ, thus $\mathbf{q} = [x, \theta]$ are the cart inverted pendulum system coordinate.The desired position can be derived as follows

$$\frac{d}{dt}\left(\frac{\partial \mathcal{L}}{\partial \dot{q}_i}\right) - \frac{\partial \mathcal{L}}{\partial q_i} = Q_i \tag{2}$$

where Q_i is the external force that applied in term of q_i coordinate. The Lagranges equation shown in Eq.(2). The total kinetic energy of the cart obtained with the movement of the cart is only in horizontal axis $\hat{\imath}$ direction as

$$K_M = \frac{1}{2} M \dot{x}^2 \tag{3}$$

where M is the mass of the cart and $\dot{x}$ is the translational velocity of the cart. The total kinetic energy of the pendulum obtained with the movement of the pendulum in the vertical and the horizontal axis ($\hat{\jmath}$ and $\hat{\imath}$) directions.

$$K_m = \frac{1}{2} m\left(\dot{x}_\theta^2 + \dot{h}^2\right) \tag{4}$$

where m is the mass of the pendulum, $\dot{h}$ is the projected pendulum position rate on the vertical axis, and $\dot{x}_\theta$ is the projected pendulum position rate on the horizontal axis. Figure.1 shows that

$$x_\theta = x + l\sin\theta \tag{5}$$

$$h = l\cos\theta \tag{6}$$

where l is the length of the pendulum rod. Eq.(5) and Eq.(6) can be derived as

$$\dot{x_\theta} = \dot{x} + l\dot{\theta}\cos\theta \tag{7}$$

$$\dot{h} = -l\,\dot{\theta}\sin\theta \tag{8}$$

By substituting Eq.(7) and Eq.(8) into Eq.(4), the kinetic energy of the pendulum can be derived as

$$K_m = \frac{1}{2} m\left(\left(\dot{x} + l\dot{\theta}\cos\theta\right)^2 + \left(-l\,\dot{\theta}\sin\theta\right)^2\right) \tag{9}$$

$$K_m = \frac{1}{2} m\left(\dot{x}^2 + 2\dot{x}l\dot{\theta}\cos\theta + l^2\dot{\theta}^2\right) \tag{10}$$

The cart and pendulum has a total kinetic energy as

$$K = K_M + K_m = \frac{1}{2} M\dot{x}^2 + \frac{1}{2} m\left(\dot{x}^2 + 2\dot{x}l\dot{\theta}\cos\theta + l^2\dot{\theta}^2\right) \tag{11}$$

The potential energy is only affected by the mass of the pendulum m

$$P = mgh = mgl\cos\theta \tag{12}$$

At last, Eq.(1) can be determined using Eq.(11) and Eq.(12), as the Lagrangian function shown as

$$\mathcal{L} = \frac{1}{2} M\dot{x}^2 + \frac{1}{2} m\left(\dot{x}^2 + 2\dot{x}l\dot{\theta}\cos\theta + l^2\dot{\theta}^2\right) \tag{13}$$

$$-mgl\cos\theta$$

The dynamics of the system must be declared in terms of θ and x as the two degrees of freedom of the system. The equation for each generalised coordinate can be derivated as follows

$$\frac{d}{dt}\left(\frac{\partial \mathcal{L}}{\partial \dot{x}}\right) - \frac{\partial \mathcal{L}}{\partial x} = f \tag{14}$$

$$\frac{d}{dt}\left(\frac{\partial \mathcal{L}}{\partial \dot{\theta}}\right) - \frac{\partial \mathcal{L}}{\partial \theta} = 0 \tag{15}$$

The equation shows that the DC motor or external force only affect the cart in $\hat{\imath}$ direction. The external force does not affects the pendulum. The differential equation from Eq.(14) and Eq.(15) can be derived as

$$\left(\frac{\partial \mathcal{L}}{\partial \dot{x}}\right) = (M+m)\dot{x} + ml\dot{\theta}\cos\theta \tag{16}$$

$$\frac{d}{dt}\left(\frac{\partial \mathcal{L}}{\partial \dot{x}}\right) = (M+m)\ddot{x} + ml\ddot{\theta}\cos\theta - ml\dot{\theta}^2\sin\theta \tag{17}$$

$$\frac{\partial \mathcal{L}}{\partial x} = 0 \tag{18}$$

and

$$\left(\frac{\partial \mathcal{L}}{\partial \dot{\theta}}\right) = ml\dot{x}\cos\theta + ml^2\dot{\theta} \tag{19}$$

$$\frac{d}{dt}\left(\frac{\partial \mathcal{L}}{\partial \dot{\theta}}\right) = ml(\ddot{x}\cos\theta - \dot{\theta}\dot{x}\sin\theta) + ml^2\ddot{\theta} \tag{20}$$

$$\frac{\partial \mathcal{L}}{\partial \theta} = -m\dot{x}l\dot{\theta}\sin\theta + mgl\sin\theta \tag{21}$$

therefore

$$f = (M+m)\ddot{x} + ml\ddot{\theta}\cos\theta - ml\dot{\theta}^2\sin\theta \tag{22}$$

$$0 = ml(\ddot{x}\cos\theta - \dot{\theta}\dot{x}\sin\theta) + ml^2\ddot{\theta} - \tag{23}$$

$$(-m\dot{x}l\dot{\theta}\sin\theta + mgl\sin\theta)$$

The equations contain nonlinear terms: terms $sin()$, $cos()$, and $\dot{\theta}^2$, therefore from Eq.(22) and Eq.(23) it can be seen that the equation represent the nonlinear of the system. The linearised Lagranges equation can be determined as

$$f = (M+m)\ddot{x} + ml\ddot{\theta} \tag{24}$$

$$0 = \ddot{x} + l\ddot{\theta} - g\theta \tag{25}$$

The pendulum assumed always rotates near the equilibrium,$\theta \approx 0$. Hence, the non linear terms can be $\sin\theta \approx \theta$, $\cos\theta \approx 1$, $\dot{\theta}^2 = 0$ and $\dot{\theta}\theta = 0$.

2.2 DC Motor

The equivalent circuit of DC motor armature shows in Figure.2.

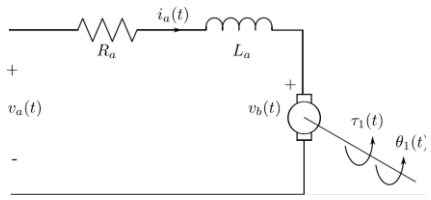


Fig. 2: Equivalent Circuit of DC Motor Armature

The equation for the DC motor armature circuit can be derived as

$$\boldsymbol{i_a R_a + L_a \frac{di_a}{dt} + v_b = v_a} \tag{26}$$

$\boldsymbol{v_b}$, the generated emf (back electromotive force) is proportional to the rotor rotational speed

$$\boldsymbol{v_b = K_b \frac{d\theta_1}{dt}} \tag{27}$$

where $\boldsymbol{K_b}$ is the constant of back emf and $\boldsymbol{\omega_1 = \frac{d\theta_1}{dt}}$. The motor torque $\boldsymbol{\tau_1}$ with the armature current $\boldsymbol{i_a}$ are proportional , hence

$$\boldsymbol{\tau_1 = K_t i_a} \tag{28}$$

where $\boldsymbol{K_t}$ is the constant of motor torque. Eq.(27) and Eq.(28) (in term of $\boldsymbol{i_a}$) substituted into Eq.(26), then

$$\boldsymbol{\frac{\tau_1}{K_t} R_a + L_a \frac{d^2\tau_1}{dt^2} + K_b \frac{d\theta_1}{dt} = v_a} \tag{29}$$

The inductor $\boldsymbol{L_a}$ can be ignored along with the small size of the inductor in the rotor, and the function of DC motor armature circuit in term of $\boldsymbol{\tau_1}$ becomes

$$\boldsymbol{\tau_1 = -K_t \frac{K_b}{R_a} \omega_1 + \frac{K_t}{R_a} v_a} \tag{30}$$

In pulley and geared systems there is the mechanical transmission applied,

$$\boldsymbol{\frac{\tau_2}{\tau_1} = \frac{N_2}{N_1} = \frac{\omega_2}{\omega_1} = \frac{r_2}{r_1}} \tag{31}$$

where $\boldsymbol{N}$ is the total amount of gear teeth and $\boldsymbol{r}$ is the pulley radius. The DC motor angular velocity $\boldsymbol{\omega_1}$ can be shown by $\boldsymbol{\dot{x}}$ as

$$\boldsymbol{\frac{2\pi r_2}{\dot{x}} = \frac{r_2}{r_1} \frac{2\pi}{\omega_1}} \tag{32}$$

where $\boldsymbol{2\pi r_2}$ is the pulley circle that links using a belt to the cart. Hence,

$$\boldsymbol{\omega_1 = \frac{\dot{x}}{r_1}} \tag{33}$$

Substituting the Eq.(33) into Eq.(30) generates

$$\boldsymbol{\tau_1 = K_r(-K_b \frac{\dot{x}}{r_1} + v_a)} \tag{34}$$

The force that caused by the torque $\boldsymbol{\tau_2}$ moves the cart, so, the transform $\boldsymbol{\tau_1 \rightarrow \tau_2}$ is needed. Hence, it can be proved that

$$\boldsymbol{f = \frac{K_r}{r_1}(-K_b \frac{\dot{x}}{r_1} + v_a)} \tag{35}$$

where $\boldsymbol{K_r = \frac{K_t}{R_a}}$. Eq.(35) and Eq.(24), makes a new term of equalised coordinate $\boldsymbol{x}$ in Lagranges function,that declared as

$$\boldsymbol{\frac{K_r}{r_1} v_a = (M + m)\ddot{x} + \frac{K_r K_b}{(r_1)^2} \dot{x} + ml\ddot{\theta}} \tag{36}$$

To simplify derivation, the abbreviations are used as follows

$$\boldsymbol{c_1 = \frac{K_r K_b}{(r_1)^2}} \tag{37}$$

$$\boldsymbol{c_2 = \frac{K_r}{r_1}} \tag{38}$$

from the Eq.36), the term $\boldsymbol{l\ddot{\theta}}$ and Eq.(25) into Eq.(36), the differential equation in a cart of the system can be derived as

$$\boldsymbol{\ddot{x} = \frac{1}{M}(c_2 v_a - c_1 \dot{x} - mg\theta)} \tag{39}$$

Rearrange Eq.(25), the equation derived as

$$\boldsymbol{\ddot{\theta} = \frac{1}{l}(g\theta - \ddot{x})} \tag{40}$$

The next differential function in the pendulum of the system can be derived from Eq.(39) and Eq.(40), as

$$\boldsymbol{\ddot{\theta} = \frac{1}{l}(g\theta - \frac{1}{M}(c_2 v_a - c_1 \dot{x} - mg\theta))} \tag{41}$$

$$\boldsymbol{= -\frac{c_2}{Ml} v_a + \frac{c_1}{Ml} \dot{x} + \frac{(M+m)g}{Ml} \theta} \tag{42}$$

Lastly, the function of the differential cart and pendulum movement using Lagranges equation has been obtained, and the dynamic actuators have been respected in the development of mathematical models.

2.3 State Space Representation

Figure.3 represents the system in state space model.

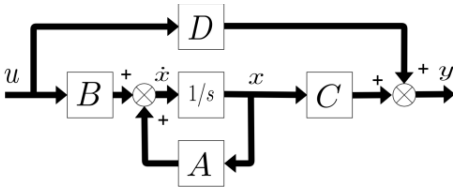


Fig. 3: Open loop system representation in state space

The representatives of state space equation can be derived as

$$\boldsymbol{\dot{x} = Ax + Bu} \tag{43}$$

$$\boldsymbol{y = Cx + Du} \tag{44}$$

where $\boldsymbol{x \in R^{n \times n}}$ is the vector of the state and $\boldsymbol{n}$ is the state variable total number. $\boldsymbol{\dot{x}}$ is the vector of state derivation. A vector $\boldsymbol{u \in R^k}$ is the control input or control vector that has $\boldsymbol{k}$ elements of control variables. The $\boldsymbol{A \in R^{n \times n}}$, $\boldsymbol{B \in R^{n \times k}}$ and $\boldsymbol{C \in R^{p \times n}}$ are the system, input and output matrices, respectively, where $\boldsymbol{p}$ is the number of output. The output of the vector is derived as $\boldsymbol{y \in R^p}$. The state vector, the derivation of the state vector and the control input of the state vector for the cart inverted pendulum system, t are declared as $\boldsymbol{x = [x\theta\dot{x}\dot{\theta}]^T}$, $\boldsymbol{\dot{x} = [\dot{x}\dot{\theta}\ddot{x}\ddot{\theta}]^T}$, $\boldsymbol{u = v_a}$ consecutively. The state variable has $\boldsymbol{n = 4}$ total number in this case. Regulating Eq.(39) and Eq.(42) into state-space form, the matrices of the system derived as

$$\boldsymbol{A = \begin{bmatrix} 0 & 0 & 1 & 0 \\ 0 & 0 & 0 & 1 \\ 0 & -\frac{mg}{M} & -\frac{c_1}{M} & 0 \\ 0 & \frac{(M+m)g}{Ml} & \frac{c_1}{Ml} & 0 \end{bmatrix}}, \boldsymbol{B = \begin{bmatrix} 0 \\ 0 \\ \frac{c_2}{M} \\ -\frac{c_2}{Ml} \end{bmatrix}}, \boldsymbol{C = \begin{bmatrix} 1 & 0 & 0 & 0 \\ 0 & 1 & 0 & 0 \end{bmatrix}},$$

$\boldsymbol{y = [x\theta]^T}$, $\boldsymbol{D = \emptyset}$

in assumption only from sensors, the actual value of $\boldsymbol{x}$ and $\boldsymbol{\theta}$ can be observed directly. Practically, the alteration from actual to the value that used for calculations is required.

3. State Feedback Control with Full-state Observer

3.1. State Feedback Control

Figure.4 shows a diagram of the control system using state feedback control. The feedback gain $\boldsymbol{K}$ in state feedback control is used to position the closed loop eigenvalues in desired locations. The main purpose of feedback control is to bring the output of the system $\boldsymbol{y}$ to tracks the desired position even though there is interference.

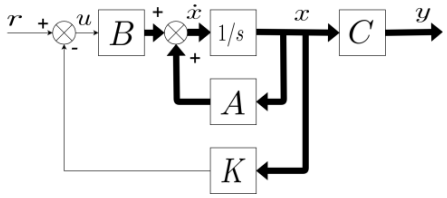


Fig. 4: Closed loop system

The system dynamic equation using state feedback control is derived as follows

$$\dot{\boldsymbol{x}} = (\boldsymbol{A} - \boldsymbol{BK})\boldsymbol{x} + \boldsymbol{Bu} \tag{45}$$

$$\boldsymbol{y} = \boldsymbol{Cx} \tag{46}$$

$$\boldsymbol{u} = \boldsymbol{r} - \boldsymbol{Kx} \tag{47}$$

where $\boldsymbol{K} \in \boldsymbol{R^j}$. Therefore, the controllability and observability of the system model checking are necessary to do before the controller is implemented. The controllability(Eq.48)) of the system means that for each initial state value, control efforts $\boldsymbol{u}$ can direct the state to each final state value in a limited time window if only $\boldsymbol{C}$ is equal to the number of state variables. Observability (Eq.49)) of the system is a property of the plant without pay attention to the selection of the actuator with suitable sensor selection. The rank of matrix $\boldsymbol{O}$ must be same with the number of the state to test that the system is a system with observability.

$$\boldsymbol{C} = [\boldsymbol{B}|\boldsymbol{AB}|\boldsymbol{A^2B}|\cdots|\boldsymbol{A^{j-1}B}] \tag{48}$$

$$\boldsymbol{O} = [\boldsymbol{C}|\boldsymbol{CA}|\boldsymbol{CA^2}|\cdots|\boldsymbol{CA^{j-1}}] \tag{49}$$

3.2. Linear Quadratic Regulator (LQR)

Linear Quadratic Regulator Controller as shown in Figure.4 is a method based on full state-feedback control. By minimising the performance cost function, the control gain **K** can be obtained, it described as

$$\boldsymbol{J} = \int_{\boldsymbol{0}}^{\infty} (\boldsymbol{x^T Q x} + \boldsymbol{u^2 R})\, \boldsymbol{dt} \tag{50}$$

where $\boldsymbol{R}$ is a scalar $\boldsymbol{Q} \in \boldsymbol{R^{j \times j}}$ is a real symmetric matrix which must be chosen. $\boldsymbol{R}$ and $\boldsymbol{Q}$ establish the relative concern of errors and energy costs. Hence, the matrix $\boldsymbol{R}$ and $\boldsymbol{Q}$ signifies a trade-off both in control efforts and performance. If $\boldsymbol{Q}$ is smaller than $\boldsymbol{R}$, control systems have become expensive since then $\boldsymbol{J}$ especially the use of the control energy. If not, when $\boldsymbol{Q}$ is bigger than $\boldsymbol{R}$, control systems become cheap because small arbitrary control efforts can be used to stabilize the system, but the system response will be slow. It is a general training to let $\boldsymbol{R} > \boldsymbol{0}$ and $\boldsymbol{Q}$ be a diagonal matrix in the form of

$$\boldsymbol{Q} = \begin{bmatrix} q_1 & 0 & \cdots & 0 \\ 0 & q_2 & \cdots & 0 \\ \vdots & \vdots & \ddots & 0 \\ 0 & 0 & \cdots & q_j \end{bmatrix} \tag{51}$$

where $(q_1, q_2, \cdots q_j)$ are greater than 0. The Laplace transfer function of the closed-loop system in Figure.4 can be used to found the denominator.

$$D(s) = s\boldsymbol{I} - (\boldsymbol{A} - \boldsymbol{BK}) \tag{52}$$

where identity matrix is $\boldsymbol{I}$. Therefore, the stability and characteristics of the transient response of the closed-loop system can be determined with all eigenvalues of $(\boldsymbol{A} - \boldsymbol{BK})$. The choosing of the feedback gain design is an effort to do, $\boldsymbol{K}$ so that the eigenvalues of $(\boldsymbol{A} - \boldsymbol{BK})$ have negative real parts. By solving the following Equation of Riccati for a positive definite matrix $\boldsymbol{P}$, the optimal feedback gain $\boldsymbol{K}$ can be obtained as

$$\boldsymbol{A^T P} + \boldsymbol{PA} - \boldsymbol{PB}R^{-1}\boldsymbol{B^T P} + \boldsymbol{Q} = 0 \tag{53}$$

and the optimal feedback gain $\boldsymbol{K}$ can be derived as

$$\boldsymbol{K} = R^{-1}\boldsymbol{B^T P} \tag{54}$$

For a unit step reference input, the transfer function $T(s)$ of a closed-loop has dc gain $N, 0 < N < 1$. The closed loop system transfer function shown in Figure.4 is declared as

$$T(s) = \boldsymbol{C}(s\boldsymbol{I} - (\boldsymbol{A} - \boldsymbol{BK}))^{-1}\boldsymbol{B} \tag{55}$$

where the dc gain N can be derived by $T(s)|_{s=0}$. $\bar{N}$ in the system is added as shown in Figure.5 can be the settlement to repair the performance of the steady state error. The pregain $\bar{N}$ is calculated as $\bar{N} = \frac{1}{N}$.

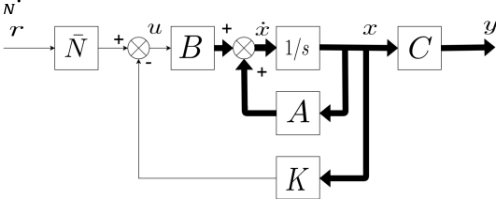


Fig. 5: Closed loop system with pregain

The equation of state space can be derived as follow, where $\boldsymbol{K} \in \boldsymbol{R^j}$.

$$\dot{\boldsymbol{x}} = (\boldsymbol{A} - \boldsymbol{BK})\boldsymbol{x} + \boldsymbol{Bu} \tag{56}$$

$$\boldsymbol{y} = \boldsymbol{Cx} \tag{57}$$

$$\boldsymbol{u} = \boldsymbol{r}\bar{\boldsymbol{N}} - \boldsymbol{Kx} \tag{58}$$

3.3. Full-state Observer

In systems with many states, it is impossible to know all information about the state. However, not all states can be sensed by sensors, and can be reversed. The system with state feedback requires an ideal sensor that has an infinite bandwidth. In fact there are no ideal sensors and sensors also have limited bandwidth. The actual observer concept is that if we do not have all the states, it is possible to estimate these states by using the system inputs and outputs. This concept can be done if observability conditions are met. The concept of the full-state observer is as shown in Figure.6.

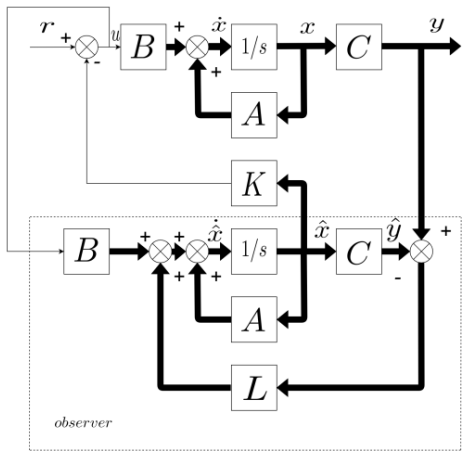


Fig. 6: Closed loop system with full-state observer

For the systems as in Eq.(43) and Eq.(44), with the state estimation of $\boldsymbol{x}$ defined as follow

$$\dot{\hat{\boldsymbol{x}}} = \boldsymbol{A}\hat{\boldsymbol{x}} + \boldsymbol{Bu} + \boldsymbol{L}(\boldsymbol{y} - \hat{\boldsymbol{y}}) \quad (59)$$

$$\hat{\boldsymbol{y}} = \boldsymbol{C}\hat{\boldsymbol{x}} \quad (60)$$

The value of $\tilde{\boldsymbol{y}} = \boldsymbol{y} - \hat{\boldsymbol{y}}$ is attempted to be as small as possible, which indicates that the estimator works well. To make $\hat{\boldsymbol{x}}$ as close as possible $\boldsymbol{x}$, state error estimator is defined.

$$\tilde{\boldsymbol{x}} = \boldsymbol{x} - \hat{\boldsymbol{x}} \quad (61)$$

$$\dot{\tilde{\boldsymbol{x}}} = \dot{\boldsymbol{x}} - \dot{\hat{\boldsymbol{x}}} \quad (62)$$

$$\dot{\tilde{\boldsymbol{x}}} = (\boldsymbol{Ax} + \boldsymbol{Bu}) - (\boldsymbol{A}\hat{\boldsymbol{x}} + \boldsymbol{Bu} + \boldsymbol{L}(\boldsymbol{Cx} - \hat{\boldsymbol{C}}\hat{\boldsymbol{x}})) \quad (63)$$

$$\dot{\tilde{\boldsymbol{x}}} = \boldsymbol{A}(\boldsymbol{x} - \hat{\boldsymbol{x}}) - \boldsymbol{LC}(\boldsymbol{x} - \hat{\boldsymbol{x}}) \quad (64)$$

$$\dot{\tilde{\boldsymbol{x}}} = (\boldsymbol{A} - \boldsymbol{LC})\tilde{\boldsymbol{x}} \quad (65)$$

One of the controller design is Output Feedback Control. By using Output Feedback Control, the existing states can be estimated using only system inputs and outputs. One method used in Output Feedback Control is to use Leuenberger estimation. By calculation

$$\boldsymbol{L} = (-\boldsymbol{S}^{-1}\boldsymbol{CP})^{\boldsymbol{T}} \quad (66)$$

where $\boldsymbol{P}$ is the solution of the Riccati equation

$$\boldsymbol{AP} + \boldsymbol{PA}^{\boldsymbol{T}} + \boldsymbol{Q} - \boldsymbol{PC}^{\boldsymbol{T}}\boldsymbol{R}^{-1}\boldsymbol{CP} = \boldsymbol{0} \quad (67)$$

In this case, the determination of the $\boldsymbol{L}$ matrix is done by the pole placement control method.

3.4. Pole Placement

In the design of the controller, the pole location of the system on the complex plane can verify the system stability . The system is unstable if it has a pole on the right side of the complex plane. In other words, the system is said to be stable when all the poles are on the left side of the complex plane[11]. Therefore, a system that has a pole in the right side of the complex plane requires a control method that can carry the pole that located in the right side of the complex plane to the left side of the complex plane. As with the previous LQR method, controllability and observability of the system must be fulfilled. The suitable gain matrix can be selected for the state feedback as shown in Figure.4, to have closed-loop poles at the desired locations, it is possible to force the system, provided that the original system completely states controllable. All the variables of state must be available and measurable in pole placement control method. The pole placement method is used to move the unstable poles to the stable poles in the left side of the complex plane such that the obtained control gain $\boldsymbol{L}$ can satisfy the designed criteria. The characteristic polynomial of the system can be derived as Eq.(68). $\boldsymbol{a_i}$ are the polynomial coefficients and $\boldsymbol{I}$ is an identity matrix. If the desired eigenvalues $\boldsymbol{\mu_1}, \cdots, \boldsymbol{\mu_n}$ are considered, the desired characteristic polynomial of the system becomes as Eq.(69). Then, the output feedback gain matrix that required $\boldsymbol{L}$ can be calculated using Eq.(70).

$$|\boldsymbol{sI} - \boldsymbol{A}| = \boldsymbol{s^n} + \boldsymbol{a_1 s^{n-1}} + \cdots + \boldsymbol{a_{n-1}s} + \boldsymbol{a_n} \quad (68)$$

$$\prod_{\boldsymbol{i=1}}^{\boldsymbol{n}}(\boldsymbol{s} - \boldsymbol{\mu_i}) = \boldsymbol{s^n} + \boldsymbol{\alpha_1 s^{n-1}} + \cdots + \boldsymbol{\alpha_{n-1}s} + \boldsymbol{\alpha_n} \quad (69)$$

$$\boldsymbol{L} = [\boldsymbol{\alpha_n} - \boldsymbol{a_n}|\boldsymbol{\alpha_{n-1}} - \boldsymbol{a_{n-1}}|\cdots|\boldsymbol{\alpha_2} - \boldsymbol{a_2}|\boldsymbol{\alpha_1} - \boldsymbol{a_1}]\boldsymbol{T^{-1}} \quad (70)$$

where $\boldsymbol{T}$ is the transformation matrix that changes the state equation of the system into the controllable canonical form. The transformation matrix $\boldsymbol{T}$ can be calculated by

$$\boldsymbol{T} = \boldsymbol{CW} \quad (71)$$

Where

$$\boldsymbol{W} = \begin{bmatrix} \boldsymbol{a_{n-1}} & \boldsymbol{a_{n-2}} & \cdots & \boldsymbol{a_1} & \boldsymbol{1} \\ \boldsymbol{a_{n-2}} & \boldsymbol{a_{n-3}} & \cdots & \boldsymbol{1} & \boldsymbol{0} \\ \vdots & \vdots & \vdots & \vdots & \vdots \\ \boldsymbol{a_1} & \boldsymbol{1} & \cdots & \boldsymbol{0} & \boldsymbol{0} \\ \boldsymbol{1} & \boldsymbol{0} & \cdots & \boldsymbol{0} & \boldsymbol{0} \end{bmatrix} \quad (72)$$

4. Simulation and Result

Before doing a simulation, the parameters of the system defined in Table 1 are used. The open loop system has the eigenvalues that shown in Figure.3 are (0, 5.3622, -5.4316, -0.3696) which can be obtained by $\det(\boldsymbol{sI} - \boldsymbol{A})$. That eigenvalue is shown in pole-zero mapping in Figure.7.

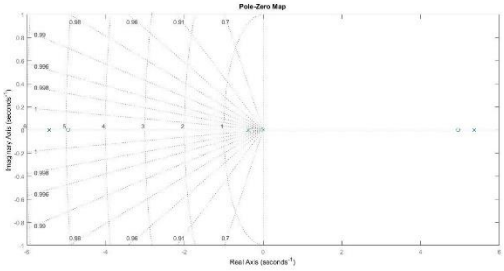


Fig. 7: Pole-Zero Mapping for a Cart Inverted Pendulum System

The open loop of cart inverted pendulum system has a positive real part or has a pole in the right side of the complex plane. Hence, the system is a system that unstable. Nevertheless, using the system state space described in Eq.(43) and Eq.(44), the cart inverted pendulum system is a completely observable and controllable. The ranks of the matrix $\boldsymbol{C}$ and $\boldsymbol{O}$ are equal to the number of the state respectively, $\text{rank}(\boldsymbol{C}) = \text{rank}(\boldsymbol{O}) = \boldsymbol{4}$, that verified using the result that shown in Eq.(73) and Eq.(74).

Table.1: The cart inverted pendulum parameters

No	Parameter	Value	Units
1	M	1.04	Kg
2	R_a	1	Ω
3	l	0.4	m
4	K_t	0.01	N.m/A
5	r_1	0.1	M
6	K_b	0.407	V.s/rad
7	m	0.19	Kg

$$\boldsymbol{C} = \begin{bmatrix} \boldsymbol{0} & \boldsymbol{0.200} & \boldsymbol{-0.008} & \boldsymbol{0.785} \\ \boldsymbol{0} & \boldsymbol{-0.800} & \boldsymbol{0.032} & \boldsymbol{-34.533} \\ \boldsymbol{0.200} & \boldsymbol{-0.008} & \boldsymbol{0.785} & \boldsymbol{-0.063} \\ \boldsymbol{-0.800} & \boldsymbol{0.032} & \boldsymbol{-34.533} & \boldsymbol{1.507} \end{bmatrix}$$

$$O = \begin{bmatrix} 1 & 0 & 0 & 0 \\ 0 & 1 & 0 & 0 \\ 0 & 0 & 1 & 0 \\ 0 & 0 & 0 & 1 \\ 0 & -0.981 & -0.040 & 0 \\ 0 & 43.164 & 0.160 & 0 \\ 0 & 0.039 & 0.002 & -0.981 \\ 0 & -0.157 & -0.006 & 43.164 \end{bmatrix}$$

4.1. State Feedback Control with Linear Quadratic Regulator

The simulation of cart inverted pendulum system of state feedback control has been obtained with a Linear Quadratic Regulator. The weighting matrix $\boldsymbol{Q}$ and $\boldsymbol{R}$ that used in 3 variations of the simulation are $\boldsymbol{q_1} = (\mathbf{1.5}, \mathbf{15})$ with the value of $\boldsymbol{q_2} = \mathbf{1}$ and $\boldsymbol{R} = \mathbf{1}$ in all combination. Figure.8 and Figure.9 shows the response of the cart position and angle pendulum respectively.

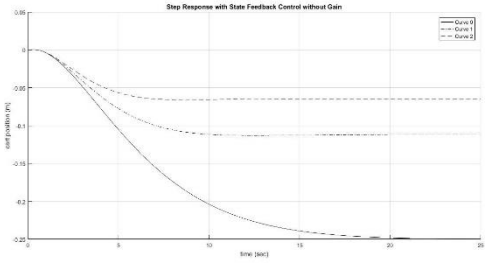


Fig. 8: Cart Position Response

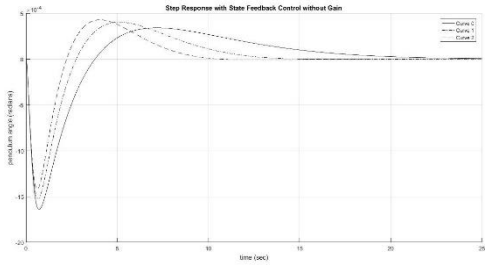


Fig. 9: Pendulum Angle Response

The cart position response shows that the cart can't reach the desired position, otherwise, the pendulum can reach the equilibrium. The bigger $\boldsymbol{q_i}$ that is given to the system, the responses become faster. Because the response of the cart that shown in Figure.8 can't reach the desired position, pregain $\bar{\boldsymbol{N}}$ added to the system for a better performance. Figure.10 and Figure.11 shows the response of the cart position and angle pendulum respectively. It can be seen that both of the cart and pendulum can reach the desired position.

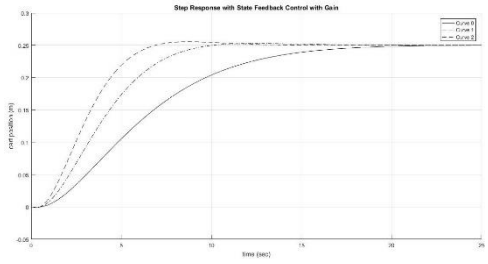


Fig. 10: Cart Position Response

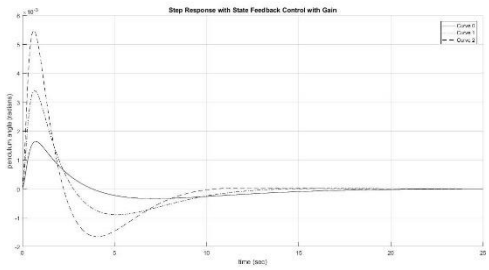


Fig. 11: Pendulum Angle Response

In this section, the simulation of the state feedback controller has been obtained.

4.2. A Full-state observer with Pole Placement

The simulation of cart inverted pendulum system using state feedback control with the full-state observer. The parameter that used in full-state observer has been obtained with pole placement control method. The pole that used for a gain matrix in Leuenberger in this simulation are (-40, -41, -42, -43). The result of the simulation also shown in Figure.10 and Figure.11. Figure.10 and Figure.11 shows the response of the cart position and angle pendulum respectively. The simulation shows that the system can reach the desired position respectively. The response with full-state observer is similar to the response with state feedback control. It because all of the state variables had been included in the mathematical model of the cart inverted pendulum system. The observer state also identical with the actual plant.

5. Conclusion

State feedback control with a full-state estimator for a cart inverted pendulum system has been successfully conducted. The gain state feedback $\boldsymbol{K}$ has been obtained using Linear Quadratic Regulator. The gain of full-state observer $\boldsymbol{L}$ also been obtained using pole placement control method. The simulation result shows that the cart inverted pendulum system can reach the desired position and angle with the optimal responses. The simulation also shows that the system using state feedback control and state feedback control with full state observer have similar responses. Its because the initial state and the observer state have same state variables in mathematical modeling. The implementation can be done to know the response of the cart inverted pendulum system on a real implementation.

Acknowledgment

The authors would like to thank Kemenristekdikti and State Polytechnic of Malang for their support.

References

[1] I. Siradjuddin, Z. Amalia, B. Setiawan, F. Ronilaya, E. Rohadi, A. Setiawan, S. Adhisuwignjo, "Stabilising a cart inverted pendulum with an augmented PID control scheme," In MATEC Web of Conferences, EDP Sciences, 2018, Vol. 197, p. 11013.

[2] I. Siradjuddin, B. Setiawan, A. Fahmi, Z. Amalia, E. Rohadi, "State space control using LQR method for a cart-inverted pendulum linearised model," International Journal of Mechanical & Mechatronics Engineering IJMME-IJENS, 2017, Vol:17, No:01

[3] I. Siradjuddin, Z. Amalia, B. Setiawan, R. P. Wicaksono and E. Yudaningtyas, "Stabilising a cart inverted pendulum system using pole placement control method," 2017 15th International Conference on Quality in Research (QiR) : International Symposium on Electrical and Computer Engineering, Nusa Dua, 2017, pp. 197-203.

[4] Zhenkai Guo, Jianqin Mao and Ping Wang, "An Approach of Adaptive Fuzzy Modeling and Application to Inverted Pendulum

Control," 2006 6th World Congress on Intelligent Control and Automation, Dalian, 2006, pp. 1594-1598.
[5] L. Ye, "Secondary Pendulum Control System Based on Genetic Algorithm and Neural Network," 2006 Chinese Control Conference, Harbin, 2006, pp. 1152-1155.
[6] E. S. Sazonov, P. Klinkhachorn and R. L. Klein, "Hybrid LQG-neural controller for inverted pendulum system," Proceedings of the 35th Southeastern Symposium on System Theory, Morgantown, WV, USA, 2003, pp. 206-210.
[7] Y. Kado, Y. Pan and K. Furuta, "Control System for Skill Acquisition- Balancing Pendulum based on Human Adaptive Mechatronics-," 2006 IEEE International Conference on Systems, Man and Cybernetics, Taipei, 2006, pp. 4040-4045.
[8] I. Park, J. Kim and J. Oh, "Online Biped Walking Pattern Generation for Humanoid Robot KHR-3(KAIST Humanoid Robot - 3: HUBO)," 2006 6th IEEE-RAS International Conference on Humanoid Robots, Genova, 2006, pp. 398-403.
[9] B. A. Sharif and A. Ucar, "State feedback and LQR controllers for an inverted pendulum system," 2013 The International Conference on Technological Advances in Electrical, Electronics and Computer Engineering (TAEECE), Konya, 2013, pp. 298-303.
[10] Z. Jie and R. Sijing, "Sliding mode control of inverted pendulum based on state observer," 2016 Sixth International Conference on Information Science and Technology (ICIST), Dalian, 2016, pp. 322-326. doi:10.1109/ICIST.2016.7483432\
[11] C. Mahapatra and S. Chauhan, "Tracking control of inverted pendulum on a cart with disturbance using pole placement and LQR," 2017 International Conference on Emerging Trends in Computing and Communication Technologies (ICETCCT), Dehradun, 2017, pp. 1-6.